

Bordetella hinzii Pneumonia in Patient with SARS-CoV-2 Infection

Hend Ben Lakhal, José Bras Cachinho, Pierre Kalfon, Thierry Naas, Zehaira Benseddik

Patients infected with severe acute respiratory syndrome coronavirus 2 might have bacterial and fungal superinfections develop. We describe a clinical case of coronavirus disease with pulmonary aspergillosis associated with *Bordetella hinzii* pneumonia in an immunocompetent patient in France. *B. hinzii* infections are rare in humans and develop secondary to immunosuppression or debilitating diseases.

Severe acute respiratory syndrome coronavirus 2 (SARS-CoV-2) has spread globally and strained health systems with an exponentially increasing number of acute respiratory failures (1). Because severe cases of respiratory distress require ventilator assisted respiration, severe bacterial and fungal co-infections can develop and lead to increased deaths (2,3). *Bordetella hinzii* is a gram-negative, aerobic coccobacillus initially described as a cause of respiratory infection in poultry and rarely in rodents (4,5). Human infections are rare and occur mostly in immunocompromised persons upon exposure to infected animals (6,7). In humans, these infections were described in 1994 in an HIV-infected patient as a cause of bacteremia (6) and have since been rarely identified in a wide range of infections (8–10). We report a clinical case of SARS-CoV-2 infection associated with pulmonary aspergillosis and *B. hinzii* pneumonia.

The Study

This case-patient was identified during routine patient care. Thus, the need for ethics approval was exempted; verbal consent was obtained from the patient.

A 63-year-old man with no notable medical history was admitted for cough, asthenia, and shortness of breath starting 3 days before admission. The patient had a positive result for a SARS-CoV-2 rapid antigen autotest. At the emergency department, COVID-19 diagnosis was confirmed by a positive SARS-CoV-2 RT-PCR result for a nasopharyngeal swab sample

Author affiliations: Centre Hospitalier de Chartres, Le Coudray, France (H. Ben Lakhal, J. Bras Cachinho, P. Kalfon, Z. Benseddik); Hôpital Bicêtre, Kremlin-Bicêtre, France (T. Naas)

DOI: <https://doi.org/10.3201/eid2804.212564>

and chest computed tomography, which showed bilateral ground-glass opacities (50% involvement) and beginning of consolidation in the lower lobes of the lungs (Figure).

He received dexamethasone (6 mg/d for 10 d), subcutaneous, low molecular weight heparin (2 × 6,000 IU/d during the entire hospitalization), ceftriaxone (2 g/d), and spiramycin (1.5 × 10⁶ IU 3×/d). On day 2 of hospitalization, he was transferred to the intensive care unit, antimicrobial drug treatment was stopped, and awake prone positioning was combined with high-flow nasal oxygen therapy.

On day 9, mechanical ventilation was applied because of acute respiratory distress syndrome, worsening hypoxemia, and gas exchange deterioration. There was no documented bacterial superinfection, and after 48 hours, the patient's oxygenation level had improved.

On day 13, respiratory function worsened; purulent aspiration and fever developed, and inflammatory markers increased (C-reactive protein 254 mg/L [reference <10 mg/L] and procalcitonin 0.35 ng/mL [reference <0.1 ng/mL]). Four-day intravenous piperacillin/tazobactam treatment (4 g/0.5 g 4×/d) was initiated, and an endotracheal aspirate (EA) showed oropharyngeal flora (10⁷ CFU/mL) and 5 × 10⁵ CFU/mL methicillin-susceptible *Staphylococcus aureus*, 5 × 10³ CFU/mL *B. hinzii*, 5 × 10² CFU/mL amoxicillin-susceptible *Escherichia coli*, and 5 × 10² CFU/mL *Candida tropicalis*.

On day 17, another EA showed oropharyngeal flora (10⁷ CFU/mL), decreased methicillin-susceptible *S. aureus* (5 × 10³ CFU/mL), increased *B. hinzii* (10⁶ CFU/mL), amoxicillin-susceptible *E. coli* (10⁷ CFU/mL), and *Aspergillus fumigatus* (10² CFU/mL). *A. fumigatus* was considered as an infection because of worsening of respiratory failure despite piperacillin/tazobactam treatment, ventilatory support for severe acute respiratory distress syndrome, an *A. fumigatus*-positive culture on EA (absent on previous EAs), and a computed tomography scan showing cavitating infiltrates (Figure). Voriconazole treatment (400 mg on the first day, followed by 200 mg/12 h) was given for 21 days, in combination with intravenous co-amoxiclav (1 g 3×/d).

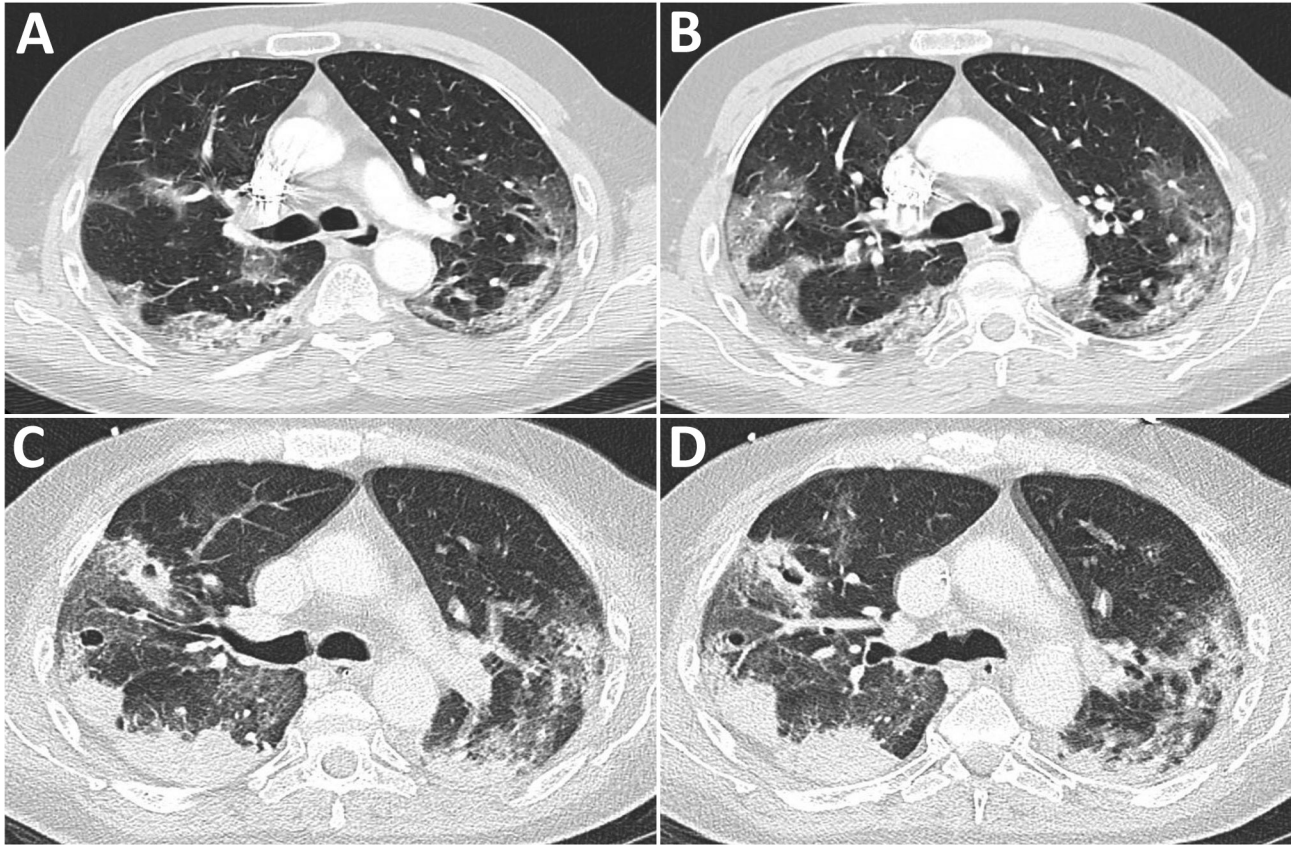


Figure. Computed tomography scans of patient with *Bordetella hinzii* pneumonia and severe respiratory syndrome coronavirus 2 infection. A, B) Scan at admission showing bilateral evidence of extensive areas of mainly crazy paving patterns with some posterior consolidations. C, D) Scan at day 25 showing marked increased extent of consolidation.

EA was repeated on day 25 because of persistence of fever, progressive clinical deterioration, and worsening of radiologic findings and showed 10^6 CFU/mL *B. hinzii*, 10^5 CFU/mL amoxicillin-susceptible *E. coli*, and 10^3 CFU/mL *C. tropicalis*, which was considered as colonization. We switched treatment to piperacillin/tazobactam (4 g/0.5 g 4×/d for 8 d), which resulted in negative results on subsequent EA samples. Testing of rectal swab samples, blood, and urine cultures remained negative throughout hospitalization. The patient was extubated on day 46 and discharged uneventfully from the hospital.

B. hinzii grew on horse blood agar (bioMérieux, <https://www.biomerieux.com>) at 37°C after incubation for 24 hours as smooth, gray colonies. We identified *B. hinzii* by using matrix-assisted laser desorption/ionization time-of-flight mass spectrometry (Biotyper; Bruker, <https://www.bruker.com>) and confirmed it by using whole-genome sequencing (Illumina, <https://www.illumina.com>) as described (11).

We initially performed antimicrobial susceptibility testing by using Etest (bioMérieux), confirmed results by using disk diffusion and broth microdilution

(Thermo Fisher Sensititer System; Thermo Fisher, <https://www.thermofisher.com>) (Table), and interpreted results by using the 2021 European Committee on Antimicrobial Susceptibility Testing pharmacokinetic/pharmacodynamic (nonspecies related) breakpoints (12). *B. hinzii* CHAR-1 showed resistance to amoxicillin, cefotaxime, aminoglycosides, and ciprofloxacin; intermediate resistance to amoxicillin/clavulanic acid and ceftazidime; and susceptibility to piperacillin/tazobactam, meropenem, and imipenem. New molecules were also tested and remained susceptible, except for ceftolozane/tazobactam (Table).

We identified β -lactamase activity by using *B. hinzii* CHAR-1 crude protein extracts as described (13). In silico analysis showed a β -lactamase, Hinzii *Bordetella* lactamase (HBL-1), which had all canonical boxes of a functional broad-spectrum class A penicillinase (13) (Appendix Figure, <https://wwwnc.cdc.gov/EID/article/28/4/21-2564-App1.pdf>). HBL-1 had 62.7% amino acid identity with BOR-1 β -lactamase from *B. parapertussis* (13). Highly related sequences (99.7%–100% amino acid identity) were identified in genome sequences of *B. hinzii* available in public databases, suggesting

Table. Antimicrobial susceptibility of *Bordetella hinzii* isolate from patient with pneumonia and severe respiratory syndrome coronavirus 2 infection, by Etest and broth microdilution*

Test and antimicrobial drug	MIC for Etest, μg/mL	MIC for BMD, μg/mL	Interpretation	EUCAST PK-PD breakpoint, mg/L†	
				S	R
Routine antibiogram					
Amoxicillin	32	ND	R	≤2	>8
Amoxicillin/clavulanic acid (2)‡	6	ND	I	≤2	>8
Ticarcillin/clavulanic acid	16	ND	I	≤8	>16
Piperacillin/tazobactam (4)‡	0.5§	<4	S	≤8	>16
Cefotaxim	>32	ND	R	≤1	>2
Ceftazidime	2	ND	S	≤4	>8
Aztreonam	>256	>32	R	≤4	>8
Cefepime	4	4	S	≤4	>8
Meropenem	0.06	0.25	S	≤2	>8
Imipenem	0.75	<1	S	≤2	>4
Ciprofloxacin	0.75	ND	R	≤0.25	>0.5
Levofloxacin	0.75	ND	I	≤0.5	>1
Amikacin	8	2	R	≤1	>1
Gentamicin	2	ND	R	≤0.5	>0.5
Tobramycin	8	>4	R	≤0.5	>0.5
Additional antimicrobial drugs tested					
Imipenem/relebactam (4)‡	ND	1	S	≤2	>2
Meropenem/vaborbactam (8)‡	ND	0.12	S	≤8	>8
Ceftazidime/avibactam (4)‡	ND	4	S	≤8	>8
Cefiderocol	ND	1	S	≤2	>2
Ceftolozane/tazobactam (4)‡	ND	8	R	≤4	>4
Tigecycline	ND	0.5	S	0.5	>0.5
Eravacycline	ND	0.12	IE	IE	IE
Fosfomycin	ND	>64	IE	IE	IE
Colistin	ND	<0.5	IE	IE	IE

*BMD, broth microdilution; EUCAST, European Committee on Antimicrobial Susceptibility Testing; I, intermediate/susceptible with high dose; IC, inhibitory concentration; IE, insufficient evidence; ND, not determined; PK/PD, pharmacokinetic/pharmacodynamic; R, resistant; S, susceptible.
†MIC breakpoints were interpreted by using EUCAST guidelines and PK-PD (nonspecies related) breakpoints (https://www.eucast.org/clinical_breakpoints).
‡Numbers in parentheses indicate the amount of inhibitor used: 2 μg/mL for clavulanic acid; 4 μg/mL for tazobactam, relebactam, and avibactam; and 8 μg/mL for vaborbactam.
§Piperacillin/tazobactam MIC was determined by using the PIP/Tazo UMIC strip (Biocentric, <https://biocentricinc.com>).

that HBL-1-like enzymes might be native to that species (Appendix Figure). MICs of aminopenicillins and carboxypenicillins might be explained by expression of HBL-1, but, as suggested for *B. parapertussis*, additional nonenzymatic β-lactam resistance mechanisms, such as impermeability, efflux, or penicillin-binding protein affinities, might be associated for *B. hinzii*. The complete genome and HBL-1 sequences have been deposited in DDBJ/EMBL (accession no. JAJTJL000000000) and GenBank (accession nos. OM212391).

The lung microbiota of deceased patients who had COVID-19 showed complex bacterial and fungal colonization by opportunistic pathogens (14). SARS-CoV-2 infection, antimicrobial drug pressure, alveolar damage, persistent lymphocytic depletion, mechanical ventilation, corticosteroid therapy, and prolonged hospital stays might predispose critically ill COVID-19 patients to opportunistic bacterial or fungal superinfection (2,14). Critically ill COVID-19 patients have the highest percentage of secondary pulmonary infections (34.5%) compared with percentages for severely ill (8.3%) and moderately ill (3.9%) COVID-19 patients (15). COVID-19-associated pulmonary aspergillosis is

a worrisome complication in critically ill patients who show increased illnesses and deaths (2). *A. fumigatus* co-infections are frequent among critically ill COVID-19 patients (2,3). Rothe et al. showed that in a group of 50 critically ill COVID-19 patients admitted to the intensive care unit, 34% were co-infected with Enterobacterales and 18% with *A. fumigatus* (15).

Human cases of *B. hinzii* infection are rare and associated mostly with immunosuppression and anterior poultry exposure (7–10). Our patient reported recent exposure to geese and ducks, which probably led to latent or chronic colonization (digestive or respiratory tract) before infection at a time when he was most vulnerable (e.g., COVID-19 and aspergillosis superinfection). Reports of patients who have *B. hinzii* infections seem to be increasing in recent years, which might reflect emergence of this pathogen or availability of better identification methods, such as matrix-assisted laser desorption/ionization time-of-flight mass spectrometry, 16S rRNA gene sequencing, and whole-genome sequencing (8). Among the few *B. hinzii* infections described, none reported *Aspergillus* infections (9).

Reported *B. hinzii* isolates were frequently multidrug resistant, including resistance to cephalosporins, aminoglycosides, and quinolones, but remained susceptible to piperacillin/tazobactam, ceftazidime, tigecycline, and meropenem (9,10). Interpretation of antimicrobial susceptibility testing is not established, and the choice of antimicrobial drugs and treatment duration are not standardized. Cases with documented pneumonia were successfully treated with piperacillin/tazobactam or cefmetazole (9). Our patient was successfully treated with piperacillin/tazobactam, but treatment with amoxicillin/clavulanic acid failed, probably because of intermediate susceptibility of *B. hinzii* to this antimicrobial drug. Our study suggests that *B. hinzii* needs to be taken into account when initiating antimicrobial drug therapy.

Conclusions

Increasing reports of invasive *B. hinzii* might indicate its emergence as a pathogen in immunocompromised patients. We describe a *B. hinzii* and *A. fumigatus* coinfection in a SARS-CoV-2-infected immunocompetent patient who had no underlying conditions but had probable transient immunosuppression caused by dexamethasone treatment and SARS-CoV-2 infection. Our study highlights the role of opportunistic infections (by fungal or rare bacterial species) in COVID-19 patients and the need to serially monitor the bacteria/fungi in the lower respiratory tract for timely personalized treatment.

Acknowledgments

We thank Panya Wissa and Emna Warzele for providing helpful discussions and the Institut Pasteur PIBNet for performing whole-genome sequencing of the bacterial isolate.

This study was supported by a grant from the Ministère de l'Éducation Nationale et de la Recherche (Université Paris-Saclay), Assistance Publique-Hôpitaux de Paris, and the Centre Hospitalier de Chartres.

About the Author

Dr. Ben Lakhal is an intensive care physician at Louis Pasteur Hospital, Le Coudray, France. Her research interests include management of severe clinical manifestations of infectious diseases in critical care.

References

- Grasselli G, Zangrillo A, Zanella A, Antonelli M, Cabrini L, Castelli A, et al.; COVID-19 Lombardy ICU Network. Baseline characteristics and outcomes of 1,591 patients infected with SARS-CoV-2 admitted to ICUs of the Lombardy Region, Italy. *JAMA*. 2020;323:1574-81. <https://doi.org/10.1001/jama.2020.5394>
- Bassetti M, Kollef MH, Timsit JF. Bacterial and fungal superinfections in critically ill patients with COVID-19. *Intensive Care Med*. 2020;46:2071-4. <https://doi.org/10.1007/s00134-020-06219-8>
- Montrucchio G, Lupia T, Lombardo D, Stroffolini G, Corcione S, De Rosa FG, et al. Risk factors for invasive aspergillosis in ICU patients with COVID-19: current insights and new key elements. *Ann Intensive Care*. 2021;11:136. <https://doi.org/10.1186/s13613-021-00923-4>
- Register KB, Kunkle RA. Strain-specific virulence of *Bordetella hinzii* in poultry. *Avian Dis*. 2009;53:50-4. <https://doi.org/10.1637/8388-070108-Reg.1>
- Jiyipong T, Morand S, Jittapalpong S, Raoult D, Rolain JM. *Bordetella hinzii* in rodents, Southeast Asia. *Emerg Infect Dis*. 2013;19:502-3. <https://doi.org/10.3201/eid1903.120987>
- Cookson BT, Vandamme P, Carlson LC, Larson AM, Sheffield JV, Kersters K, et al. Bacteremia caused by a novel *Bordetella* species, "*B. hinzii*". *J Clin Microbiol*. 1994;32:2569-71. <https://doi.org/10.1128/jcm.32.10.2569-2571.1994>
- Fabre A, Dupin C, Bénézit F, Goret J, Piau C, Jouneau S, et al. Opportunistic pulmonary *Bordetella hinzii* infection after avian exposure. *Emerg Infect Dis*. 2015;21:2122-6. <https://doi.org/10.3201/eid2112.150400>
- Kattar MM, Chavez JF, Limaye AP, Rassoulian-Barrett SL, Yarfitz SL, Carlson LC, et al. Application of 16S rRNA gene sequencing to identify *Bordetella hinzii* as the causative agent of fatal septicemia. *J Clin Microbiol*. 2000;38:789-94. <https://doi.org/10.1128/JCM.38.2.789-794.2000>
- Maison-Fomotar M, Sivasubramanian G. *Bordetella hinzii* pneumonia and bacteremia in a patient with SARS-CoV-2 infection. *Emerg Infect Dis*. 2021;27:2904-7. <https://doi.org/10.3201/eid2711.211468>
- Collercandy N, Petillon C, Abid M, Descours C, Carvalho-Schneider C, Mereghetti L, et al. *Bordetella hinzii*: an unusual pathogen in human urinary tract infection. *J Clin Microbiol*. 2021;59:e02748-20. <https://doi.org/10.1128/JCM.02748-20>
- Jousset AB, Bonnin RA, Takissian J, Girlich D, Mihaila L, Cabanel N, et al. Concomitant carriage of KPC-producing and non-KPC-producing *Klebsiella pneumoniae* ST512 within a single patient. *J Antimicrob Chemother*. 2020;75:2087-92. <https://doi.org/10.1093/jac/dkaa137>
- European Committee on Antimicrobial Susceptibility Testing. PK-PD (non-species related) breakpoint [cited 2022 Jan 31]. https://www.eucast.org/fileadmin/src/media/PDFs/EUCAST_files/Breakpoint_tables/v_11.0_Breakpoint_Tables.pdf
- Lartigue MF, Poirel L, Fortineau N, Nordmann P. Chromosome-borne class A BOR-1 beta-lactamase of *Bordetella bronchiseptica* and *Bordetella parapertussis*. *Antimicrob Agents Chemother*. 2005;49:2565-7. <https://doi.org/10.1128/AAC.49.6.2565-2567.2005>
- Fan J, Li X, Gao Y, Zhou J, Wang S, Huang B, et al. The lung tissue microbiota features of 20 deceased patients with COVID-19. *J Infect*. 2020;81:e64-7. <https://doi.org/10.1016/j.jinf.2020.06.047>
- Rothe K, Feihl S, Schneider J, Wallnöfer F, Wurst M, Lukas M, et al. Rates of bacterial co-infections and antimicrobial use in COVID-19 patients: a retrospective cohort study in light of antibiotic stewardship. *Eur J Clin Microbiol Infect Dis*. 2021;40:859-69. <https://doi.org/10.1007/s10096-020-04063-8>

Address for correspondence: Hend Ben Lakhal, Service de Réanimation, Centre Hospitalier de Chartres, 4 Rue Claude-Bernard, 28630 Le Coudray, France; email: h.lakhal@gmail.com

Bordetella hinzii Pneumonia in Patient with SARS-CoV-2 Infection

Appendix

```

BOR-1  MNRRTFGAGMLAALGAACMPFWARAGVRRARFADAAAQAQRQLALLEQRHGARLGVQVQ  60
PBL-1  MDRRTFGAGVLAWLGASAAGLPALAGVRDLSL--AAGDDAQRQLARLEAREGGRLGVSL  58
HBL-1  MDRRTFGAGVLAWLGASAAGLPALAGVRDLSL--AASDDAQRQLARLEAREGGRLGVSL  58
HBL-2  MDRRTFGAGVLAWLGASAAGLPALAGVRDLSL--AASDDAQRQLARLEAREGGRLGVSL  58
HBL-3  MDRRTFGAGVLAWLGASAAGLPALAGVRDLSL--AASDDAQRQLARLEAREGGRLGVSL  58
      *:* *:* *:* *:* *:* *:* *:* *:* *:* *:* *:* *:* *:* *:* *:* *:* *:* *:* *:* *:* *:* *:*
      *:* *:* *:* *:* *:* *:* *:* *:* *:* *:* *:* *:* *:* *:* *:* *:* *:* *:* *:* *:* *:*

BOR-1  DRDSGGAFSHRADERFPLCSTFKLLAAAVALRADRGDDSLARLIRYGATDIVAYSFVTG  120
PBL-1  DVQSGYAIAYRADERFALCSTFKLLAVGAVLTVARGEDDLSRPMRLSAADIVTYSFVTQ  118
HBL-1  DVQSGYAIAYRADERFALCSTFKLLAVGAVLTVARGEDDLSRPMRLSAADIVDYSFVTQ  118
HBL-2  DVQSGYAIAYRADERFALCSTFKLLAVGAVLTVARGEDDLSRPMRLSAADIVDYSFVTQ  118
HBL-3  DVQSGYAIAYRADERFALCSTFKLLAVGAVLTVARGEDDLSRPMRLSAADIVDYSFVTQ  118
      *:* *:* *:* *:* *:* *:* *:* *:* *:* *:* *:* *:* *:* *:* *:* *:* *:* *:* *:* *:* *:*
      *:* *:* *:* *:* *:* *:* *:* *:* *:* *:* *:* *:* *:* *:* *:* *:* *:* *:* *:* *:* *:*
      S70 K73

BOR-1  PRQAEGMTLEQCEAAVTRSDNTAGNLLSTLGGPPGLTAYARGLDGDRVTRLDRIETALN  180
PBL-1  QRLNEGMTLGQCEAALLWGDNTAANLLSTLGGPPGLTAYARALGDGVTRLDRLEETALN  178
HBL-1  QRLNEGMTLGQCEAALLWGDNTAANLLSTLGGPPGLTAYARALGDGVTRLDRLEETALN  178
HBL-2  QRLNEGMTLGQCEAALLWGDNTAANLLSTLGGPPGLTAYARALGDGVTRLDRLEETALN  178
HBL-3  QRLNEGMTLGQCEAALLWGDNTAANLLSTLGGPPGLTAYARALGDGVTRLDRLEETALN  178
      *   *   *   *   *   *   *   *   *   *   *   *   *   *   *   *   *   *   *   *   *   *
      *   *   *   *   *   *   *   *   *   *   *   *   *   *   *   *   *   *   *   *   *   *
      S130 N136                               R164 E166

BOR-1  EARPGDPRDTPAAMAGNLERLLGDALQPASRQRLADWLLASRTGDTRLRAGLPSGWR  240
PBL-1  EARPGDERDTPAAMGNLRQLVLDVLPAPERERLRDWMQCRGTGRERLRAGLPAAWA  238
HBL-1  EARPGDERDTPAAMGNLRQLVLDVLPAPERERLRDWMQCRGTGQQLRAGLPAGWS  238
HBL-2  EARPGDERDTPAAMGNLRQLVLDVLPAPERERLRDWMQCRGTGQQLRAGLPASWS  238
HBL-3  EARPGDERDTPAAMGNLRQLVLDVLPAPERERLRDWMQCRGTGQQLRAGLPAGWS  238
      ***** ***** *:* *:* *:* *:* *:* *:* *:* *:* *:* *:* *:* *:* *:* *:* *:* *:*
      ***** ***** *:* *:* *:* *:* *:* *:* *:* *:* *:* *:* *:* *:* *:* *:* *:* *:*
      D179

BOR-1  IGDKTGAGGNGTNDVGVIPRDGAPVLITAYLTQSSASRETQNAVLAEVGRIAAHAVAA  300
PBL-1  LAHRSGAGGHGSCNDIGVAWPAPAAPVLI SAYLTESPLDLPGREVRVLAEEAARILAHALVS  298
HBL-1  LGHRTGAGGHGTCNDIGVAWPTPTTPVVISVYLTESPLDLPGREVRVLAEEAARILAHALAS  298
HBL-2  LGHRTGAGGHGTCNDIGVAWPTPTTPVVISVYLTESPLDLPGREVRVLAEEAARILAHALAS  298
HBL-3  LGHRTGAGGHGTCNDIGVAWPTPTTPVVISVYLTESPLDLPEREVRVLAEEAARILAHALAS  298
      *:* *:* *:* *:* *:* *:* *:* *:* *:* *:* *:* *:* *:* *:* *:* *:* *:* *:* *:* *:* *:*
      *:* *:* *:* *:* *:* *:* *:* *:* *:* *:* *:* *:* *:* *:* *:* *:* *:* *:* *:* *:* *:*
      R/K234

BOR-1  WRLGG- 305
PBL-1  ARLHAG 304
HBL-1  ARLHAG 304
HBL-2  ARLHAG 304
HBL-3  ARLHAG 304
      * *
  
```

Appendix Figure. Sequence alignment of β -lactamases BOR-1 from *Bordetella parapertussis* (WP_033463656 [1]); PBL-1 (*Pseudohinzii* *Bordetella* Lactamase) from *B. pseudohinzii* (WP_068945286), HBL-1 from *B. hinzii* CHAR-1 (this study, accession number pending and WP_080700357.1), HBL-2 from *B. hinzii* (WP_142176586.1), and HBL-3 from *B. hinzii* (WP_029580329.1). Conserved boxes in class A β -lactamases are indicated by black boxes, residues involved in hydrolysis or substrate stabilization in the active site are highlighted in gray, and the Omega loop is underlined (2). Amino acid differences among *B. hinzii* β -lactamases are indicated in bold. S130G substitution has been shown to be involved in inhibitor resistance (3).

References

1. Lartigue MF, Poirel L, Fortineau N, Nordmann P. Chromosome-borne class A BOR-1 beta-Lactamase of *Bordetella bronchiseptica* and *Bordetella parapertussis*. *Antimicrob Agents Chemother.* 2005;49:2565–7. [PubMed https://doi.org/10.1128/AAC.49.6.2565-2567.2005](https://doi.org/10.1128/AAC.49.6.2565-2567.2005)
2. Verma D, Jacobs DJ, Livesay DR. Variations within class-A β -lactamase physiochemical properties reflect evolutionary and environmental patterns, but not antibiotic specificity. *PLOS Comput Biol.* 2013;9:e1003155. [PubMed https://doi.org/10.1371/journal.pcbi.1003155](https://doi.org/10.1371/journal.pcbi.1003155)
3. Cantón R, Morosini MI, de la Maza OM, de la Pedrosa EG, De la Pedrosa EG. IRT and CMT beta-lactamases and inhibitor resistance. *Clin Microbiol Infect.* 2008;14(Suppl 1):53–62. [PubMed https://doi.org/10.1111/j.1469-0691.2007.01849.x](https://doi.org/10.1111/j.1469-0691.2007.01849.x)